Text S1. Calculation of $\Delta^{17}O(SO_4^{2-})$ in the model

The oxygen isotopic composition of sulfate ($\Delta^{17}O(SO_4^{2-})$) in the model is calculated as follows:

$$\Delta^{17}O\left(SO_4{}^{2-}\right) = \frac{C_{\mathrm{cloud,H_2O_2}} \times 0.7 + C_{\mathrm{cloud,O_3}} \times 9.75 + C_{\mathrm{het,H_2O_2}} \times 0.7 + C_{\mathrm{het,O_3}} \times 9.75}{C_{\mathrm{gas}} + C_{\mathrm{cloud}} + C_{\mathrm{het}} + C_{\mathrm{primary}}}$$

where C_{gas}, C_{cloud}, C_{het}, C_{primary} respectively represents sulfate concentration from gas-phase oxidation of SO_2, aqueous phase oxidation of S(IV) in clouds, heterogeneous oxidation of SO_2 on aerosol surfaces, and primary sulfate. The assumed $\Delta^{17}O(SO_4^{2-})$ value for each sulfate production pathway is summarized in Table S1.

In contrast to previous studies (e.g., He et al., 2017), we assume that the terminal oxygen atom is transferred to S(IV) during oxidation based on Liu et al. (2001), leading to higher $\Delta^{17}O(SO_4^{2-})$ values than those when assuming all three oxygen atoms of ozone are equally likely to be transferred to the product sulfate.

Table S1. $\Delta^{17}O(SO_4^{2-})$ value for each sulfate production pathway used in the GEOS-Chem model[1]

Sulfate formation pathway		$\Delta^{17}O(SO_4^{2-})$ ‰
Gas	SO_2+OH	0
In Cloud	S(IV)+H_2O_2	0.7
	S(IV)+O_3	9.75[a]
	S(IV)+TMI	0
On aerosol surface (Heterogeneous)	S(IV)+H_2O_2	0.7
	S(IV)+O_3	9.75
	S(IV)+TMI	0
	S(IV)+NO_2	0
Primary sulfate		0

[1] $\Delta^{17}O(SO_4^{2-})$ values are based on results from Savarino et al. (2000) and Liu et al (2001) and assuming $\Delta^{17}O(O_3)$ = 26‰ (Vicars et al., 2014) and $\Delta^{17}O(H_2O_2)$ = 1.4‰ (Savarino and Thiemens, 1999).

Text S2. Influence of aerosol pH on reaction probability and sulfate production rate

Figure S1 shows the calculated reaction probability (γ, Section 2) and sulfate production rate (R) as a function of aerosol pH for the four heterogeneous sulfate production mechanisms implemented into the model (TMI, O_3, H_2O_2 and NO_2) plus two additional pathways, heterogeneous S(IV) oxidation by HOBr and O_2 on acidic microdroplets as proposed by Hung and Hoffmann (2015). Concentrations used in the calculations shown in Figure S1 represent the HPP conditions: [SO_2(g)] = 20 ppb, [NO_2(g)] = 85 ppb, [O_3(g)] = 11 ppb, [H_2O_2(g)] = 0.3 ppb, [HOBr(g)] = 0.1 ppt, total soluble Fe and Mn are estimated to 10 and 20 ng m^{-3}. Concentrations of H_2O_2 and HOBr are from the standard model simulation, and all others are from observations. The mass accommodation coefficients (α in Eq. (3) in the main text) for SO_2, NO_2, O_3, H_2O_2, and HOBr are 0.23, 2×10^{-4} (Jacob, 2000), 2×10^{-3} (Jacob, 2000), 0.11, and 0.6 (Chen et al., 2016), respectively. Aerosol radius (a in Eq. (1)) and total aerosol surface area (A in Eq. (1)) depend on the type of aerosol. Here we use a =1.5×10^{-5}cm (Cheng, et al., 2016) and A =l2×10^{-5} cm^2 cm^{-3}.

As shown in Figure S1, the calculated reaction probabilities (γ) and sulfate production rates (R) are strongly pH dependent for the different sulfate formation pathways, with the exception of the H_2O_2 pathway. The calculated γ for H_2O_2 oxidation is on the order of 10^{-4} for all aerosol pH values. The lack of pH dependence for S(IV) oxidation by H_2O_2 is due to the competing effects of increases in the pseudo-first order reaction rate constant with [H^+] (the reaction is acid catalyzed) and decreasing SO_2 solubility with decreasing pH. The reaction probabilities and sulfate production rates for O_3 and NO_2 pathways increase with increasing pH because of the increase in the effective Henry's law constant of SO_2 with pH, and are limited by mass transport across the air water interface at high pH values (pH > 7). TMI-catalyzed oxidation plays an important role when pH < 4 due to the increased solubility of Fe and Mn at low pH. Heterogeneous sulfate production rates calculated as first order in SO_2 or oxidant concentrations result in similar values when aerosol

pH < 6, and are limited by the mass transport across the air-water interface at higher pH values. Calculated γ ranges from 8×10^{-6}–7×10^{-4} over all aerosol pH values, consistent with the γ values used in previous studies (Cheng et al., 2016; Zheng et al., 2015). Figure S1 also shows calculated $\Delta^{17}O(SO_4^{2-})$ for sulfate produced via heterogeneous production pathways. Calculated heterogeneous $\Delta^{17}O(SO_4^{2-})$ is lower than 0.1‰ when pH < 4, is about 0.6‰ when pH is between 3 and 5, and increases rapidly to 4.5‰ for pH of 5-7.

The reaction probability γ for the HOBr pathway is limited by mass transfer when pH > 5 due to the large aqueous-phase rate-coefficient for this reaction. Although the γ values for heterogeneous oxidation by HOBr are high (on the order of 10^{-1} as shown in Figure S1), the sulfate production rate is relatively low due to low HOBr concentrations (0.1 ppt) in the model. Chen et al. (2017) showed that HOBr concentrations were likely underestimated in GEOS-Chem; however, HOBr observations in China are not available for comparison with model results shown here. Due to the estimated low reaction rate for heterogeneous sulfate production via oxidation by HOBr and the lack of relevant observational constraints, we do not further consider this reaction pathway in this study. We note that this should be revisited in the future when observational constraints on HOBr abundance become available.

The heterogeneous sulfate production rate for SO_2 oxidation by O_2 on acidic microdroplets is very large due to calculated high γ values (resulting from the large aqueous-phase rate constant in Hung and Hoffman (2015)) and SO_2 concentrations (Figure S1). Implementation of this heterogeneous sulfate formation pathway into GEOS-Chem results in 95% of total, global, tropospheric sulfate formation occurring via this pathway (figure not shown), even though it only occurs in the model when calculated aerosol pH is lower than 3. This result seems highly unrealistic, and thus we do not consider it further here.

Table S2 Aqueous-phase reaction rate expressions, rate constants (k) and influence of ionic strength (I_s) on the first-order aqueous-phase sulfate production in aerosol.

Oxidants	k (s^{-1})	Uptake Gas	References
O_3	$k_1[H_2SO_3]+k_2[HSO_3^-]+k_3[SO_3^{2-}]$ $k_1 = 2.4\times10^4$ M^{-1} s^{-1} $k_2 = 3.7\times10^5\times\exp(-5530\times(1/T-1/298))$ M^{-1} s^{-1} $k_3 = 1.5\times10^9\times\exp(-5280\times(1/T-1/298))$ M^{-1} s^{-1}	O_3	Hoffmann and Calvert (1985)
H_2O_2	$k_4[H^+][HSO_3^-]/(1+K[H^+])$ $k_4 = 7.45\times10^7\times\exp(-4430\times(1/T-1/298))$ M^{-1} s^{-1} $K = 13$ M^{-1}	H_2O_2	McArdle and Hoffmann (1983)
NO_2	$k_5[S(IV)]$ $k_{5low} = 2\times10^6$ M^{-1} s^{-1} $k_{5high} = (1.24 - 2.95)\times10^7$ M^{-1} s^{-1}	NO_2	Seinfeld and Pandis (2012) Lee and Schwartz (1983) Clifton, C. L. (1988)
TMI + O_2	$k_6[H^+]^{-0.74}[Mn(II)][Fe(III)]$ (pH ≤ 4.2) $k_6 = 3.72\times10^7\times\exp(-8431.6\times(1/T-1/297))$ M^{-2} s^{-1} $k_7[H^+]^{0.67}[Mn(II)][Fe(III)]$ (pH > 4.2) $k_7 = 2.51\times10^{13}\times\exp(-8431.6\times(1/T-1/297))$ M^{-2} s^{-1}	SO_2	Ibusuki and Takeuchi (1987)
	$\log(k / k^{I_s=0})=b_4\sqrt{I_s}/(1+\sqrt{I_s})$ $I_{s,\,max} = 2$ M b_1 is in range of -4 to -2		Martin (1991) Martin and Hill (1967)
HOBr	$k_8[HSO_3^-]+k_9[SO_3^{2-}]$ $k_8 = 3.2\times10^9$ $M^{-1}s^{-1}$ $k_9 = 5.0\times10^9$ $M^{-1}s^{-1}$	HOBr	Chen et al. (2017)
O_2 on acidic microdroplet	1.5×10^6 (pH ≤ 3)	SO_2	Hung and Hoffmann (2015)

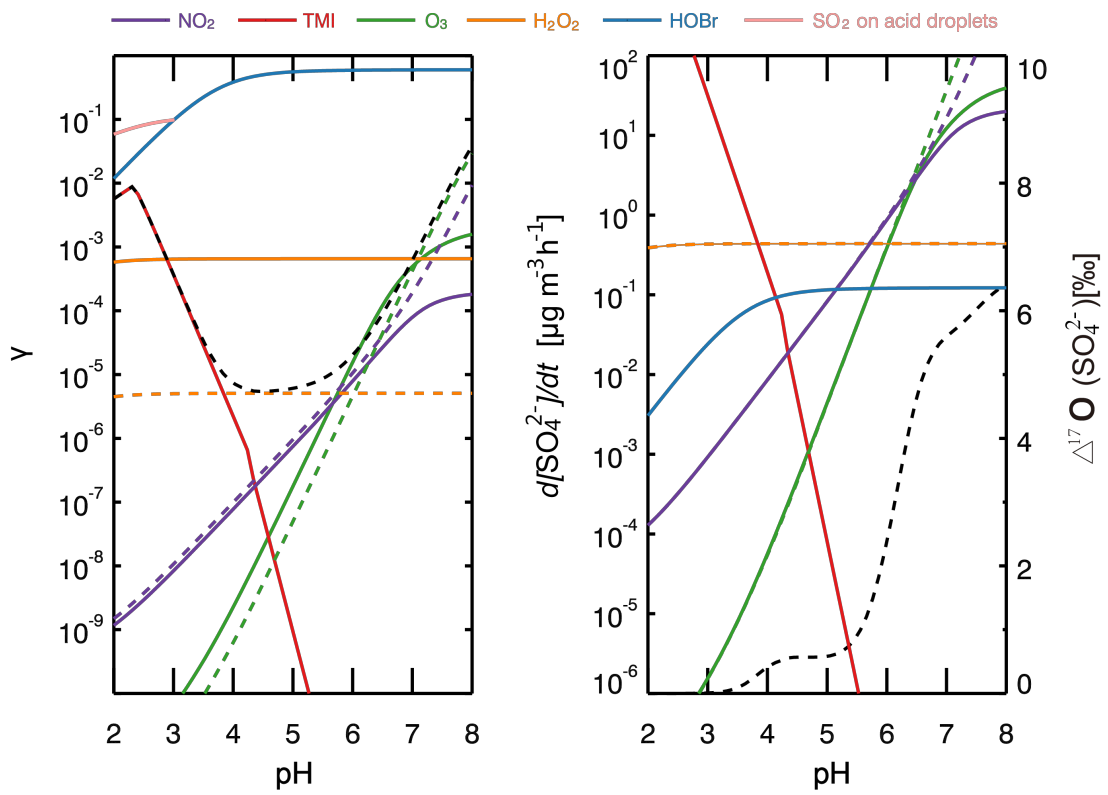

Figure S1. The dependence of reaction probability γ (left) and sulfate production rates (μg m^{-3} h^{-1}) (right) on aerosol pH for different heterogeneous sulfate formation pathways, including NO_2 (purple), TMI (red), O_3 (green), H_2O_2 (orange), HOBr (blue), and SO_2 on acid droplets (pink). The sulfate production rate on acid droplets is not shown on the figure on the right because it is off scale. The solid lines are calculated as first order in the oxidant, and the dashed lines are calculated as first order in SO_2. The black dashed line on the left represents the sum of TMI, O_3, H_2O_2 and NO_2. The black dashed line on the right represents the calculated $\Delta^{17}O(SO_4^{2-})$ value for the four reactions of TMI, O_3, H_2O_2 and NO_2.

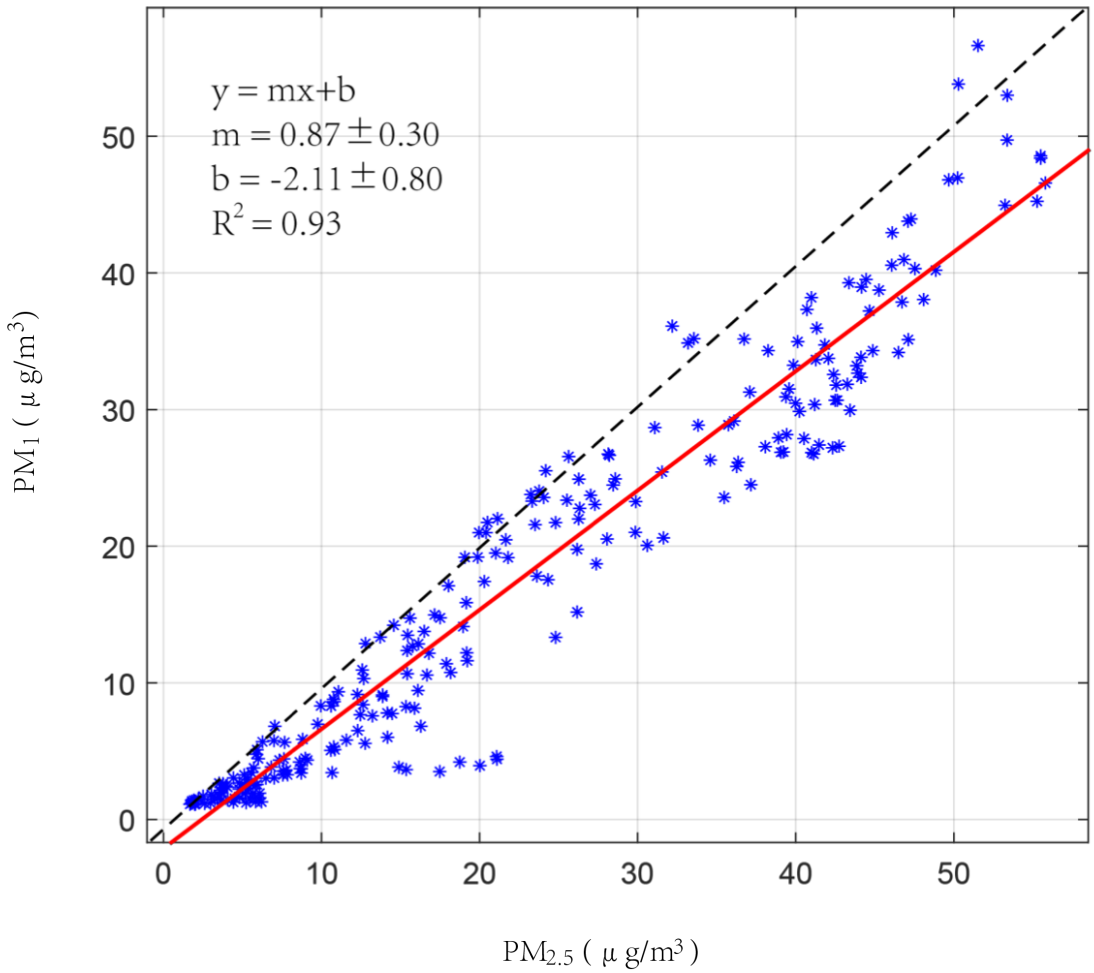

Figure S2. The relationship between sulfate concentrations in $PM_{2.5}$ and PM_1 measured in Beijing.

100

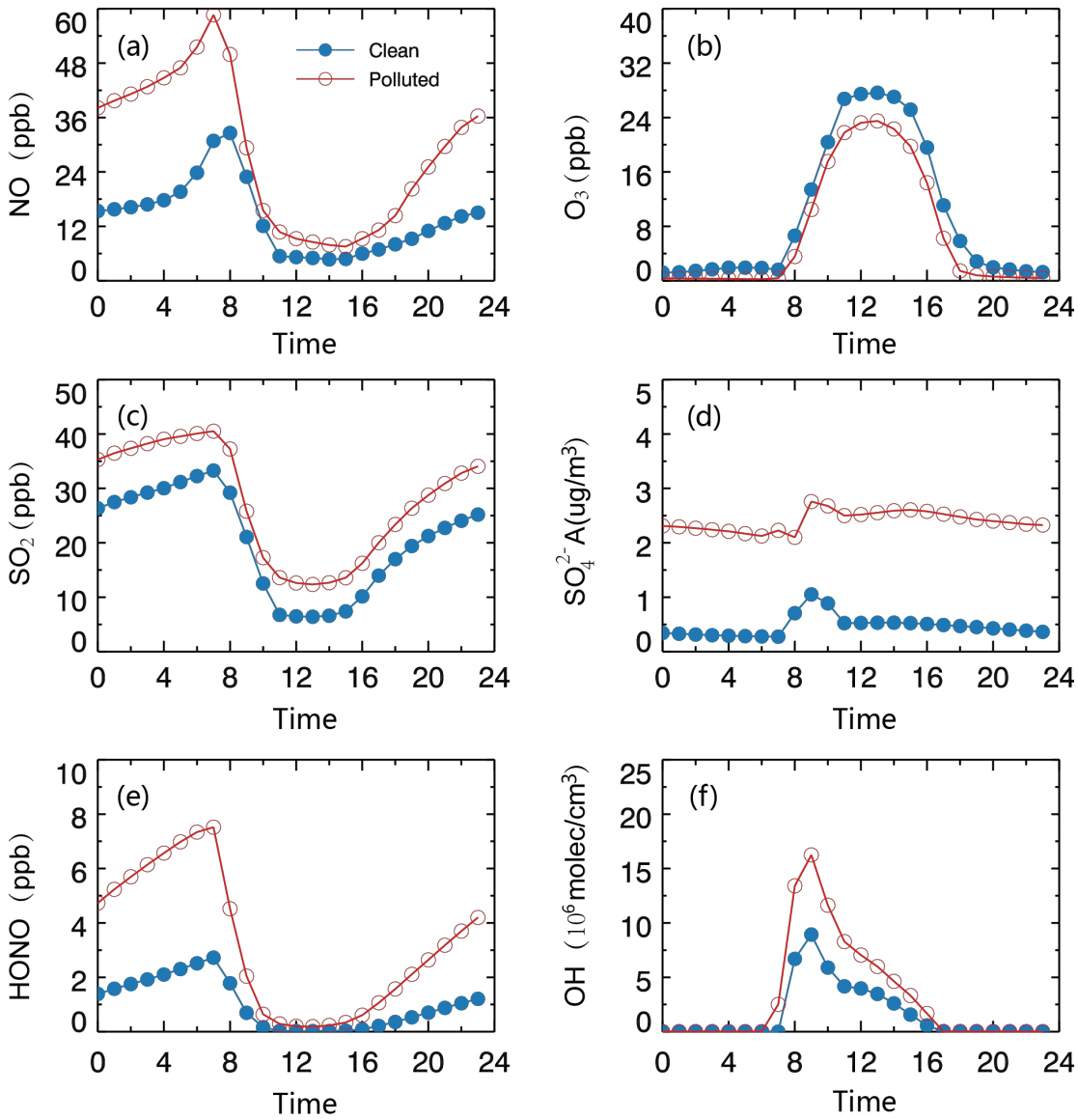

Figure S3. Modeled diurnal cycles of surface NO, O_3, SO_2, SO_4^{2-} aerosol oxidation by the SO_2 + OH pathway (SO_4^{2-}A), HONO, and OH abundances in Beijing. The red lines denote averages for heavy polluted periods and the blue lines denote averages for clean periods as defined in the text.

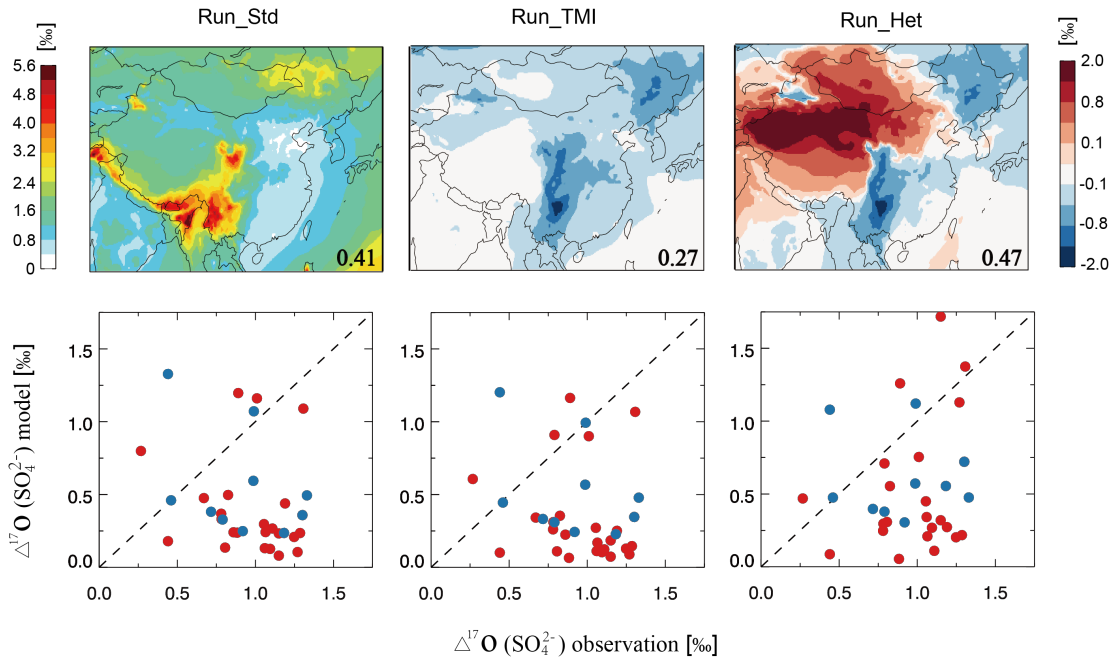

Figure S4. Modeled $\Delta^{17}O(SO_4^{2-})$ and comparisons with observations in Beijing. The top panels show modeled spatial distribution of $\Delta^{17}O(SO_4^{2-})$ over Asia averaged over the measurement period. The top left panel shows simulated $\Delta^{17}O(SO_4^{2-})$ in Run_Std; the middle and right panels show differences relative to Run_Std in Run_TMI and Run_Het, respectively. Numbers in inset are simulated mean $\Delta^{17}O(SO_4^{2-})$ values (‰) in Beijing averaged over the entire collection period. The bottom panels show observed vs. modeled $\Delta^{17}O(SO_4^{2-})$ in Beijing in Run_Std (left), Run_TMI (middle), and Run_Het (right) separated for heavy pollution (HPP; red circles) and clean (CP; blue circles) periods.

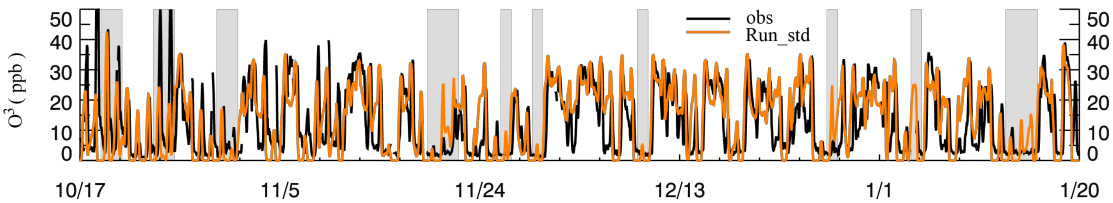

Figure S5. Time series of O_3 at the surface in Beijing during the study period of 17 October 2014 – 20 January 2015. Hourly O_3 observations (black line) are compared with model results from Run_Std (orange line). The gray shaded bars represent 10 heavy pollution periods (HPP) as defined in the text.

References

Liu, Q., L. M. Schuerter, C. E. Muller, S. Aloisio, J. S. Francisco, and D. W. Margerum (2001), Kinetics and mechanisms of aqueous ozone reactions with bromine, sulfite, hydrogen sulfite, iodide, and nitrite ions, Inorg. Chem., 40, 4436-4442.

Hoffmann, M. R. & Calvert, J. G. Chemical Transformation Modules for Eulerian Acid Deposition Models: Volume II, the Aqueous-phase Chemistry. Atmospheric Sciences Research Laboratory, Office of Research and Development, US Environmental Protection Agency, 1985.

McArdle, J. V. & Hoffmann, M. R. Kinetics and mechanism of the oxidation of aquated sulfur dioxide by hydrogen peroxide at low pH. J. Phys. Chem. 87, 5425-5429 ,1983.

Seinfeld, J. H. & Pandis, S. N. Atmospheric chemistry and physics: From air pollution to climate change. John Wiley & Sons, 2012.

Lee, Y. N. & Schwartz, S. E. in Precipitation scavenging, dry Deposition and resuspension. 453-470 ,Elsevier, 1983.

Clifton, C. L., Altstein, N. & Huie, R. E. Rate constant for the reaction of nitrogen dioxide with sulfur (IV) over the pH range 5.3-13. Environ. Sci. Technol. 22, 586-589 , 1988.

Ibusuki, T. & Takeuchi, K. Sulfur dioxide oxidation by oxygen catalyzed by mixtures of manganese (II) and iron (III) in aqueous solutions at environmental reaction conditions. Atmos. Environ. 21, 1555-1560 , 1987.

Martin, L. R. & Hill, M. W. The iron catalyzed oxidation of sulfur: Reconciliation of the literature rates. Atmos. Environ. 21, 1487-1490 ,1967.

Martin, L., Hill, M., Tai, A. & Good, T. The iron catalyzed oxidation of sulfur (IV) in aqueous solution: differing effects of organics at high and low pH. J. Geophys. Res. 96, 3085-3097 ,1991.

Hung, H.-M. & Hoffmann, M. R. Oxidation of gas-Phase SO2 on the surfaces of acidic microdroplets: Implications for sulfate and sulfate radical anion formation in the atmospheric liquid phase. Environ. Sci. Technol. 49, 13768-13776 ,2015.

Chen, Q., Geng, L., Schmidt, J. A., Xie, Z., Kang, H., Dachs, J., Cole-Dai, J., Schauer, A. J., Camp, M. G., and Alexander, B.: Isotopic constraints on the role of hypohalous acids in sulfate aerosol formation in the remote marine boundary layer, Atmospheric Chemistry and Physics, 16, 11433-11450, 10.5194/acp-16-11433-2016, 2016.

Vicars, W. and J. Savarino (2014). "Quantitative constraints on the ^{17}O-excess (□^{17}O) signature of surface ozone: Ambient measurements from 50°N to 50°S using the nitrite-coated filter technique." Geochem. Cosmochem. Acta 135: 270-287.

Savarino, J. and M. H. Thiemens (1999b). "Analytical procedure to determine both □^{18}O and □^{17}O of H_2O_2 in natural water and first measurements." Atmos. Env. 33: 3683-3690.